



SHARIF UNIVERSITY OF TECHNOLOGY  
**Advance Neuroscience**

Dr.Ali Ghazizadeh

**Assignment 1**

By:Mohammad Khorshidi

## 1 Integrate and Fire Model

1. As we know  $\lambda$  in Poisson point process serves as firing rate in Poisson like neurons. So I generate some Poisson spike trains with  $\lambda = 100$  and  $\Delta\tau = 1$  ms. You can see the raster plot in Figure 1.

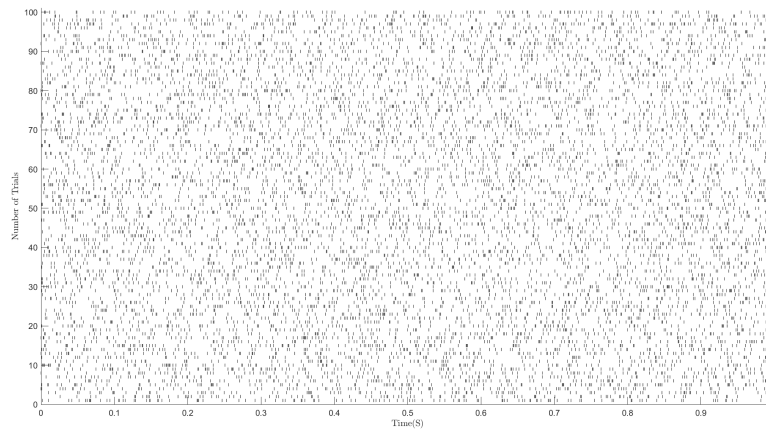


Figure 1: Poisson Like Neuron Raster Plot

2. With generating a lot of trials of Poisson point process and plot the firing rate pdf, so we can compare the ideal pdf with the some trials the generated point process. It can be seen in Figure 2.

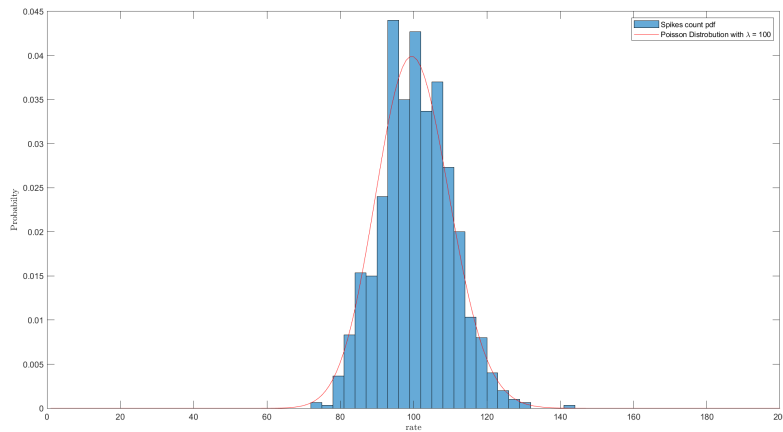


Figure 2: Poisson Like Neuron Spike Count pdf vs Ideal Poisson pdf

3. For interspike intervals, first computing the histogram of the times from generated data, then compare it with the ideal pdf of exponential distribution; because we know that interspike interval of Poisson like

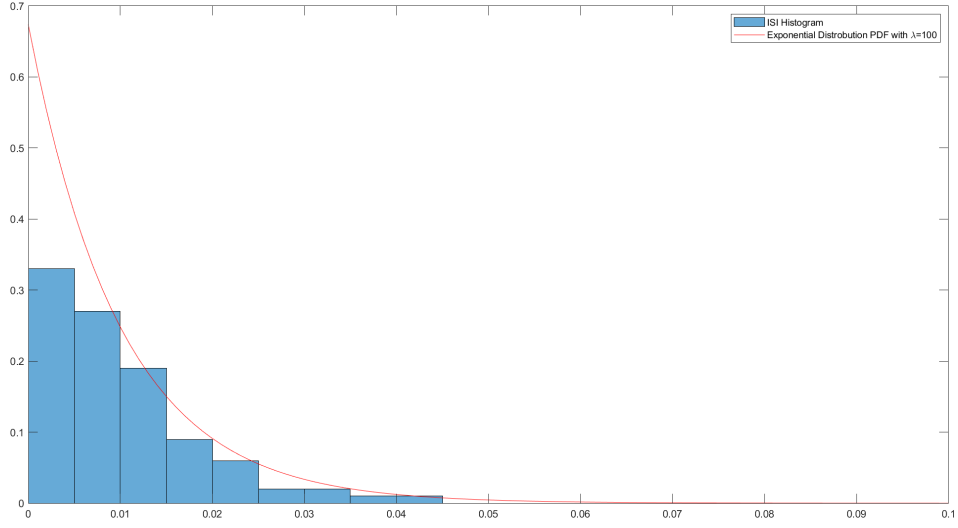
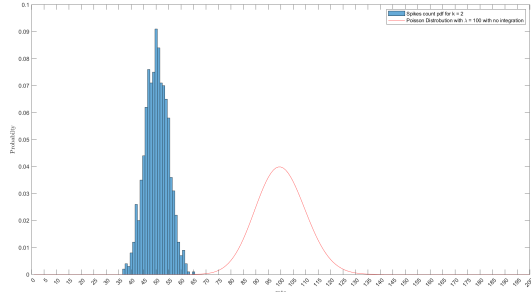


Figure 3: Poisson Like Neuron Interspike Intervals Generated pdf vs Ideal Exponential pdf

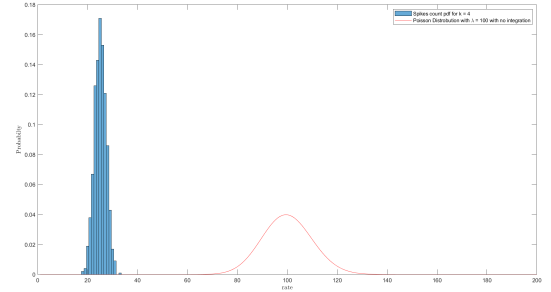
neuron is exponential distribution. It can be seen in Figure 3.

### Renewal Process

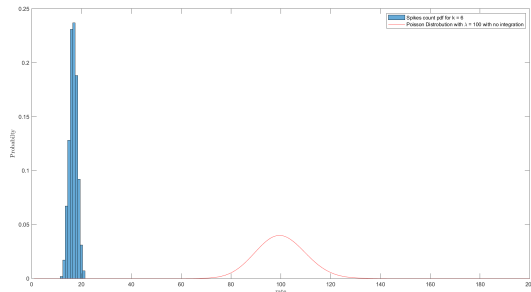
- For this approach, first I generate a Poisson point process spike train, then choose the  $k$ th spike in every trial to show a renewal process that waits until the  $k$ th spike arrives and then fires. It is just like the time when a neuron integrates  $k$  spikes to fire itself. In Figure 4 you can see the difference between the renewal process and a Poisson point process. It can be seen that the peak of the distribution is shifted to  $\lambda/k$  and is bigger than the usual Poisson point process. Another critical point is that the variability of spike counts seems to be decreased. It is because the essence of an integration system; reduces variability.



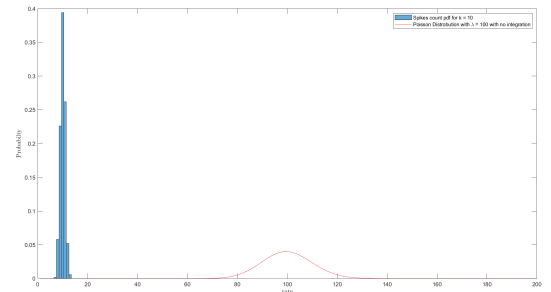
(a)  $k = 2$



(b)  $k = 4$



(c)  $k = 6$



(d)  $k = 10$

Figure 4: Different Renewal Point Processes Compare to usual Poisson Point Process

- For ISI, we know that summation over  $k$  independent exponential distribution with parameter  $\lambda$  will be an Erlang distribution with parameters  $\lambda$  and  $k$ . It can be compared to exponential distribution and Erlang

distribution in Figure 5

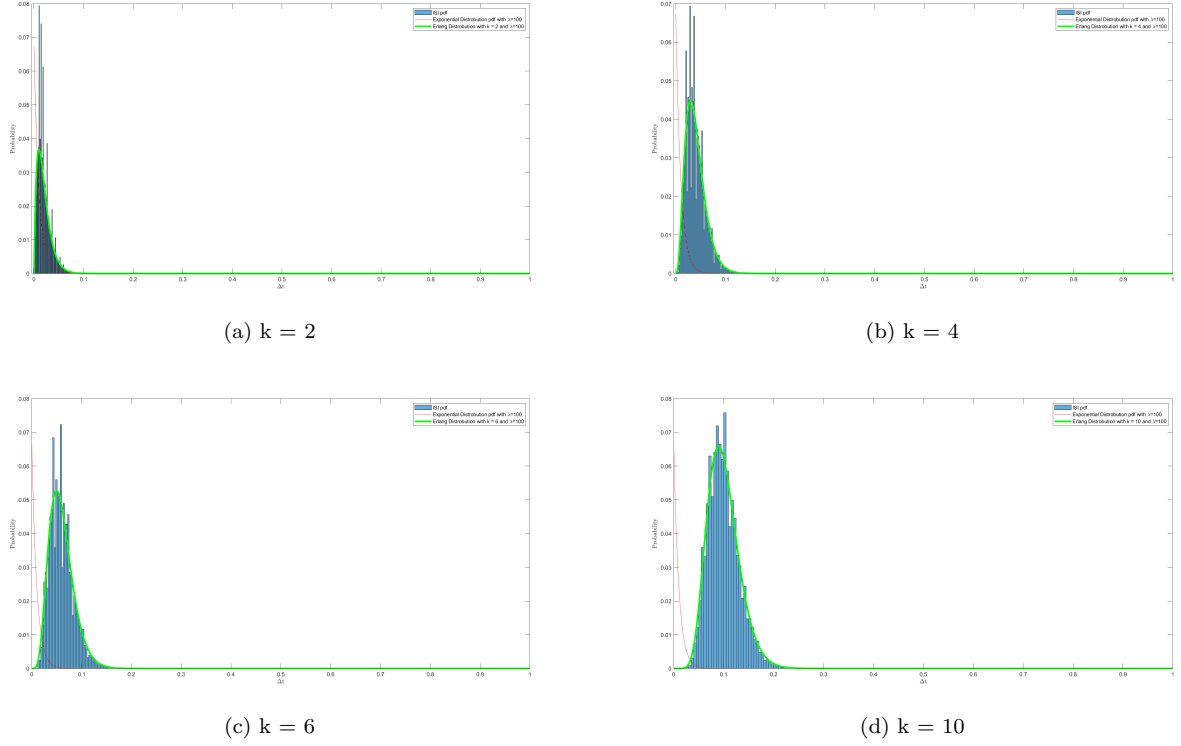


Figure 5: Different Renewal Point Processes ISIs Compare to usual Poisson Point Process ISI and ideal Erlang distribution.

6. Here we have to compute the coefficient of variation of the generated data for different renewal processes. As we know, the formulation for computing the  $C_v$  is  $\frac{std(\tau)}{\mathbb{E}(\tau)}$  where  $\tau$  is the ISIs. It is expected that when there is an integration, the variability of the process is reduced, and if we see Figure 6 we can see this. In theory, we know that the ISI of a Poisson point process comes from an exponential distribution, because:  $\tau \sim Exponential(\lambda)$ ;  $var(\tau) = \mathbb{E}(\tau) = \lambda$ . And if we sum over independent random variables which come from the same Exponential distribution, with the same parameter  $\lambda$ , it will result in a random variable that comes from distribution and is called Erlang distribution. This distribution has two parameters.

$$X_i \sim Exp(\lambda) \Rightarrow \tau = \sum_{i=1}^k X_i, \quad \tau \sim Erlang(k, \lambda) \quad \text{Erlang's pdf} \Rightarrow f(x; k, \lambda) = \frac{\lambda^k x^{k-1} e^{-\lambda x}}{(k-1)!} \quad \text{for } x, \lambda \geq 0$$

We have for Erlang distribution  $\Rightarrow$

$$C_v = \frac{std(\tau)}{\mathbb{E}(\tau)} = \frac{(\frac{\sqrt{k}}{\lambda})}{(\frac{k}{\lambda})} = \frac{1}{\sqrt{k}}$$

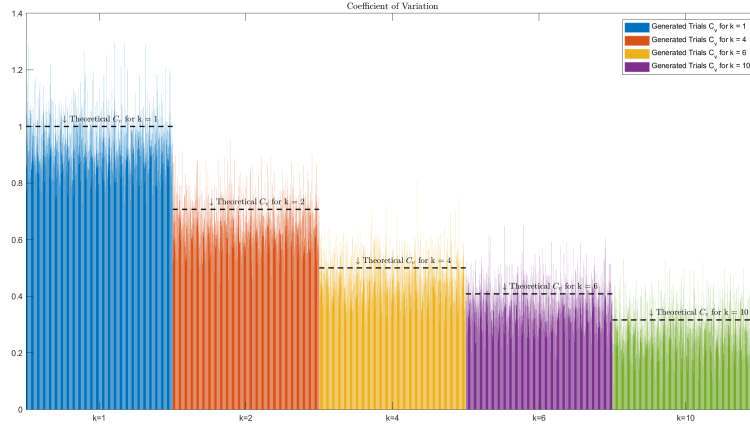


Figure 6: Different Renewal Processes Coefficient of Variation from generated Data vs Theoretical Expectation.

7. Here I am trying to give a mathematical proof for Erlang distribution's Pdf.

- (a) If  $X$  and  $Y$  are independent random variables with probability density functions  $f$  and  $g$ , then  $X + Y$  has density:

$$(f * g)(x) = \int_0^x f(\tau)g(x - \tau)d\tau$$

- (b) Let  $T_i$  be independent random variables which comes from same Exponential distribution with parameter  $\lambda$ ;

$$f(x) = \lambda e^{-\lambda x}; x \geq 0$$

We have for  $T_1 + T_2$ :

$$(f * f)(x) = \int_0^x f(\tau)f(x - \tau)d\tau$$

$$(f * f)(x) = \lambda^2 e^{-\lambda x}$$

For  $T_1 + T_2 + T_3$  we have:

$$(f * f * f)(x) = (f * f_2)(x) = \frac{\lambda^3 x^2}{2} e^{-\lambda x}$$

So for  $T_1 + T_2 + T_3 + \dots + T_k$  we have:

$$(f * f_{k-1}) = \frac{\lambda^k x^{k-1} e^{-\lambda x}}{(k-1)!}$$

$$\mathbb{E}[f_k(x)] = \int_0^x f_k(x)dx = \int_0^x \frac{\lambda^k x^{k-1} e^{-\lambda x}}{(k-1)!} = \frac{k}{\lambda}$$

$$std[f_k(x)] = \sqrt{var[f_k(x)]} \Rightarrow$$

$$var[f_k(x)] = \mathbb{E}[f_k(x)^2] - \mathbb{E}[f_k(x)]^2 = \frac{(k+1)k}{\lambda^2} - \frac{k^2}{\lambda^2} = \frac{k}{\lambda^2}$$

$$C_v = \frac{std[f_k(x)]}{\mathbb{E}[f_k(x)]} = \frac{1}{\sqrt{k}}$$

8. As we know, the refractory period impacts the firing rate variability, because when the rate is high enough, the refractory period doesn't allow neurons to fire more variable and the firing rate becomes more stable and neuron fires periodic; so there is just one rate were the neuron fire at it. As Softky and Koch showed in their paper [1], the real data showed these properties and it can be seen in Figure 7.

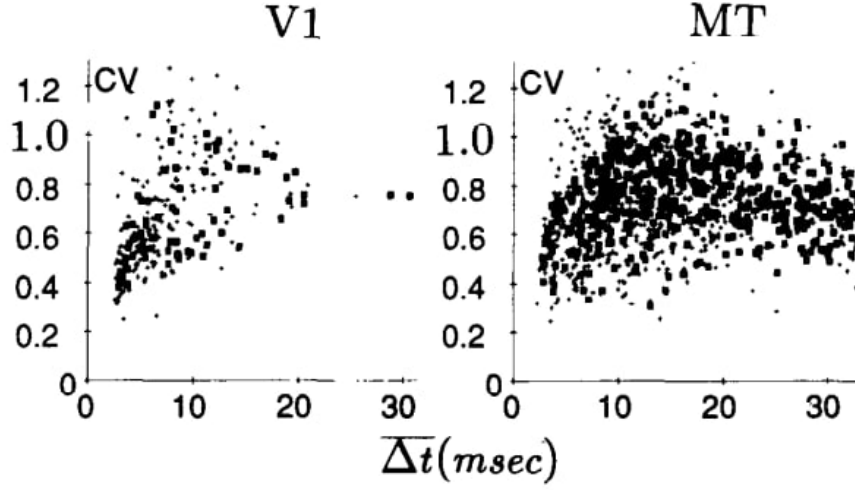


Figure 7: Variability of neurons in areas V1 and MT.

For generated data, It can be seen from Figure 8 that for high firing rate, the variability is near zero and for smaller rates, it tends to their values when there is no refractory period. It can be seen that even 1ms refractory period affects variability a lot.

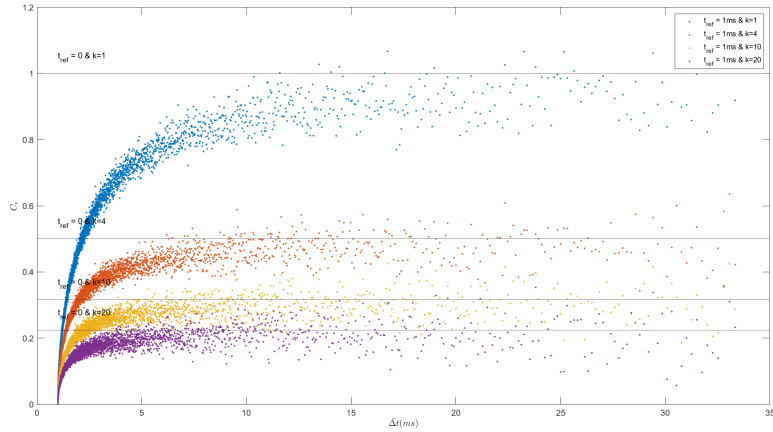


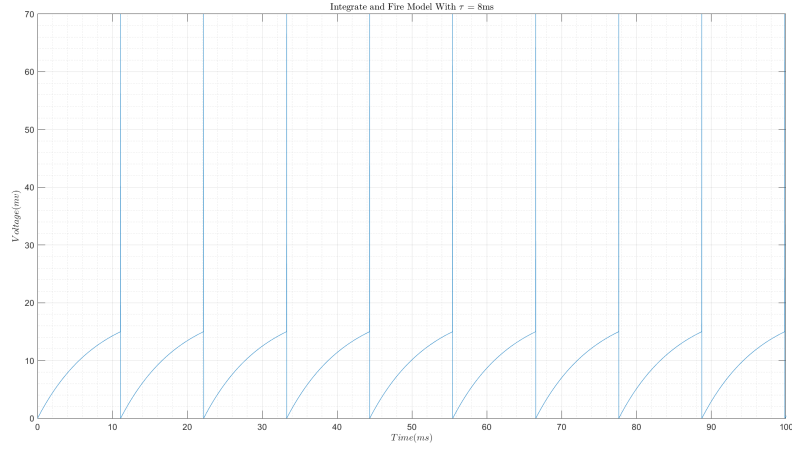
Figure 8: Refractory Period Impacts on Firing Rate Variability

## 2 Leaky Integrate and Fire Model

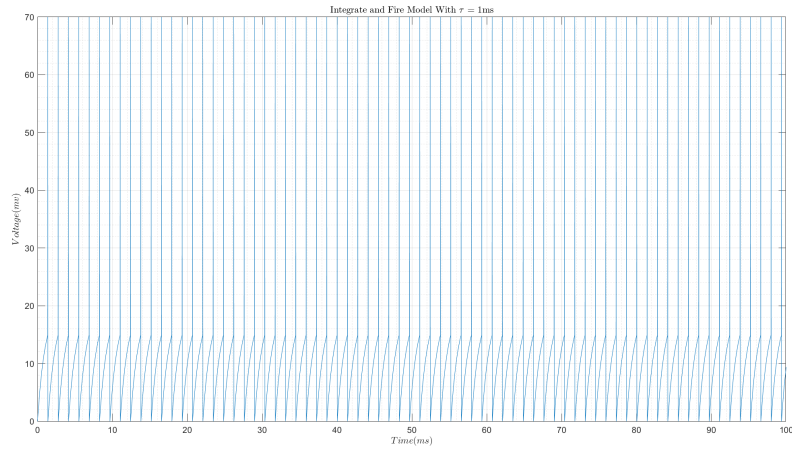
1. With the following model for neural firing, the neuron voltage during time for different  $\tau_m$ s can be seen in Figure 9.

The Model:

$$\tau_m \frac{dv}{dt} = -v(t) + RI(t)$$



(a)  $\tau_m = 8 \text{ ms}$



(b)  $\tau_m = 1 \text{ ms}$

Figure 9: Membrane Voltage at the Time  $t$  With Different  $\tau_m$ .

2. If  $v(t)$  doesn't reach  $v_{th}$ :

$$v(t) = RI(1 - \exp(\frac{-t}{\tau_m}))$$

In  $t = t_0$ ,  $v(t) = v_{th}$ :

$$v(t_0) = v_{th} = RI(1 - \exp(\frac{-t_0}{\tau_m})) \Rightarrow$$

$$\frac{RI - v_{th}}{RI} = \exp(\frac{-t_0}{\tau_m}) \Rightarrow t_0 = -\tau_m \ln \frac{RI - V_{th}}{RI} \Rightarrow$$

$\delta_{tr} \triangleq \text{Refractory Period}$

$$T = t_0 + \delta_{tr} \Rightarrow f = \frac{1}{T} = \frac{1}{\tau_m \ln \frac{RI - V_{th}}{RI} + \delta_{tr}}$$

3. Here with the help of the LIF for the time-varying input current  $I(t)$ . formulation, and the current kernel, first, I generate the current to give it to the input of the neuron and then, if the voltage goes over threshold, it will be fired.

The LIF formulation for a time varying  $I(t)$ :

$$v(t) = v_r \exp(-\frac{t - t_0}{\tau_m}) + \frac{R}{\tau_m} \int_0^{t-t_0} \exp(-\frac{s}{\tau_m}) I(t-s) ds$$

I assumed  $v_r = 0$  ( $v_{t0}$ ) and  $t_0 = 0$ . The Current kernel:

$$I_s(t) \propto t \exp(-\frac{t}{t_{peak}})$$

Accordingly:

$$I(t) = \sum_i \delta(t - t_i) \cdot I_s(t)$$

where  $t_i$  is the time of  $i$ th synaptic input spike.

We can see an example of a neuron which is working with above formulation in Figure 10 and the input current and current kernel in Figure 11. The width of current kernel is 15 ms and the  $t_{peak}$  is at 1.5 ms.

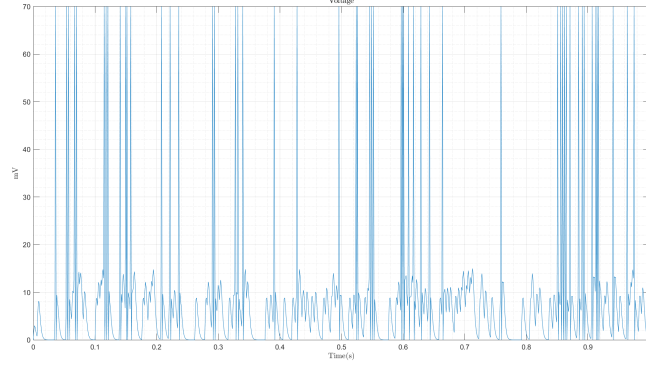
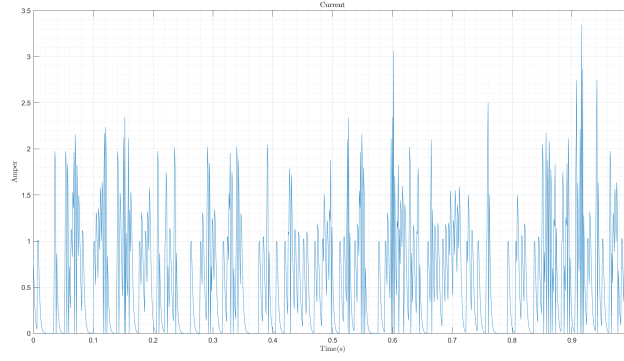
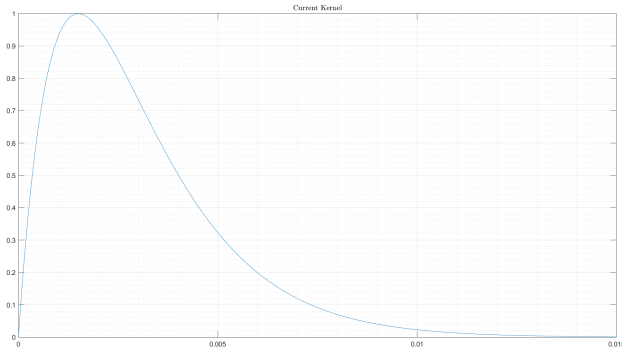


Figure 10: Voltage of a Neuron With LIF Formulation with Time Varying  $I(t)$



(a) The Synaptic Current  $I(t)$



(b) The Current Kernel

Figure 11: The Time Varying  $I(t)$

The Softky and Koch in [1] tried to calculate the CV with different  $N_{th}$  and  $\tau_m$ . They wanted to show that for a coincidence detector Neuron, the CV is near 1 even when the number of inputs that neuron needs to fire is more than 1. We can see the CV contour plot form [1] in Figure 12.

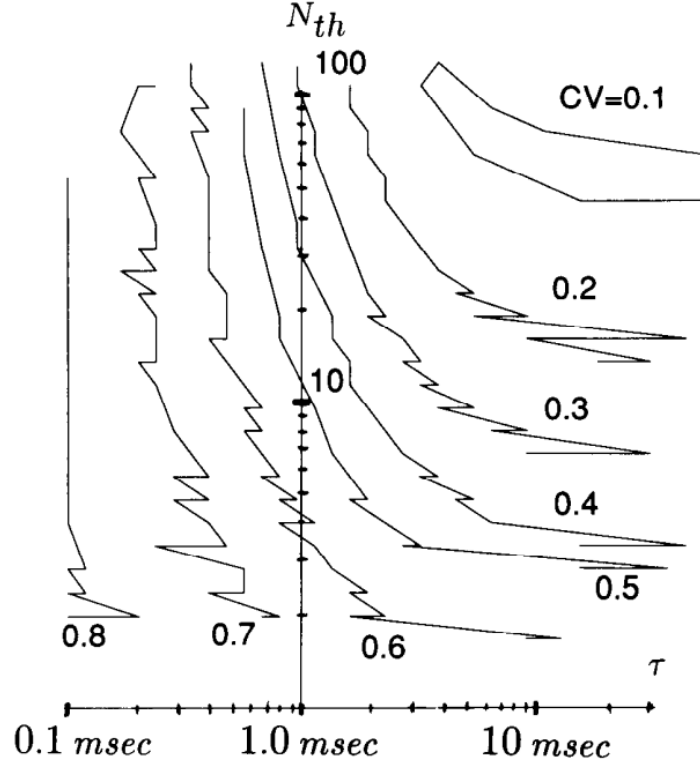


Figure 12: The Softky and Koch Simulation CVs.

I then try to regenerate the contour plot 12, and I ended with 13. As we can see, if Neuron become an integrator neuron with bigger  $N_{th}$ , the CV is decreasing more. Another important thing we can get from the plot is that if the neuron is a coincidence detector (the smaller  $\tau_m$  the neuron will be more coincidence detector.) And the bigger  $\tau_m$ , the smaller CV.

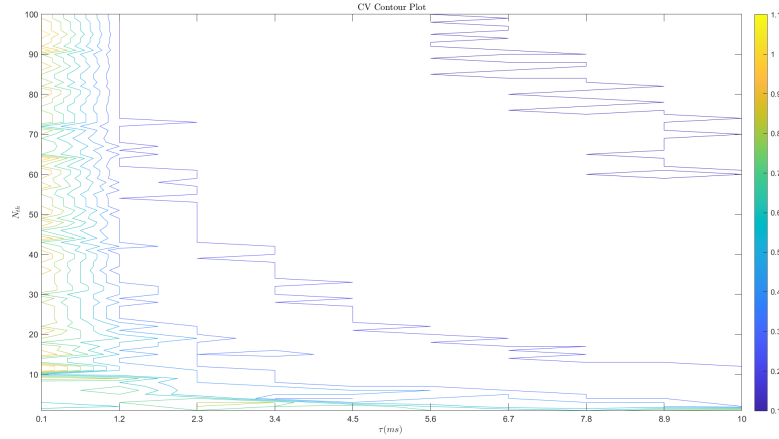


Figure 13: CV Contour Plot for Different  $\tau_m$  and  $N_{th}$ .

To see the effect of the magnitude and the width of the current kernel, I do a simulation to see the result. As we can see in Figure 14, the bigger width results to bigger CV. Also another simulation is done to see the affect of Magnitude and the  $t_{peak}$ . As we can see in Figure 15, the bigger  $t_{peak}$  and magnitude, the bigger CV.



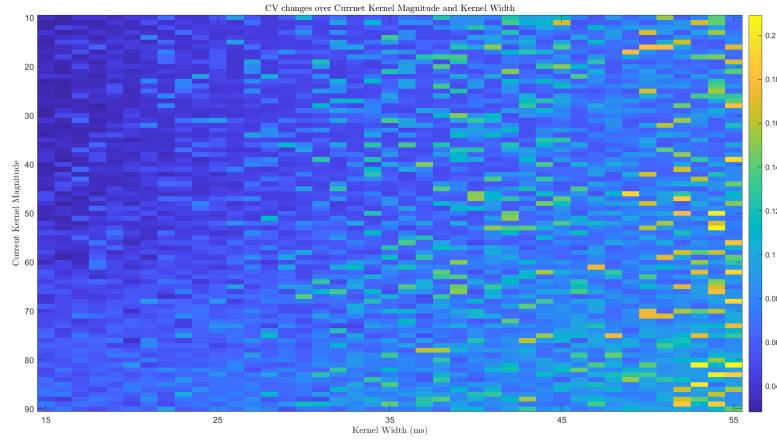


Figure 14: CV Changes over Magnitude and Current Kernel Width.

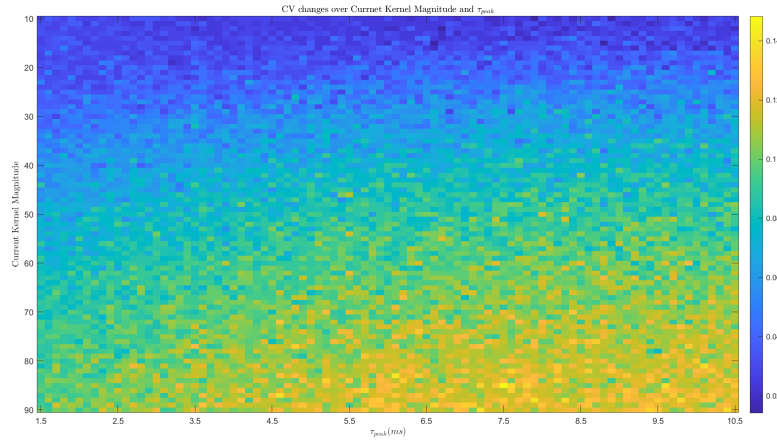
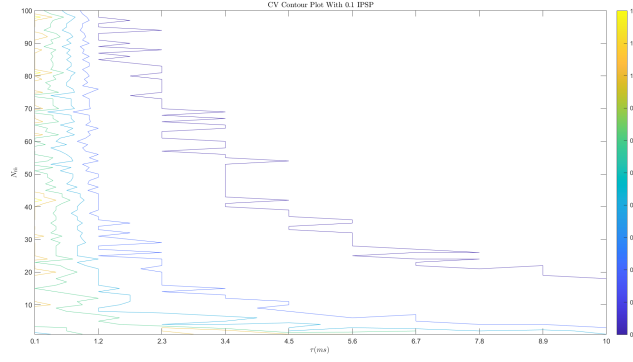
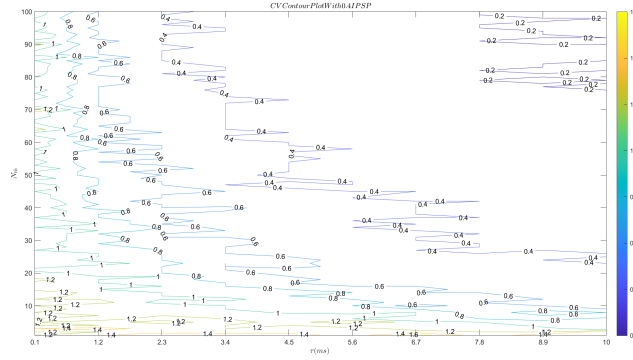


Figure 15: CV Changes over Magnitude and  $t_{peak}$  of Current Kernel.

4. As Shadlen and Newsom showed in their work [shadlen], there is no effort for neurons to be coincidence detectors to have CV near 1. If some of the input of Neuron be inhibitory, the CV can get closer to 1 and even be bigger than 1. So in here, I forced the inputs to be inhibitory so we can see the effect of IPSPs on the CV. As we can see in Figure 16, the more percentage the IPSPs, the more CV. Also we can see it in 17.



(a) CV Contour Plot for IPSP Percentage = 10



(b) CV Contour Plot for IPSP Percentage = 40

Figure 16: CV contour Plot for Different Percentage of IPSPs

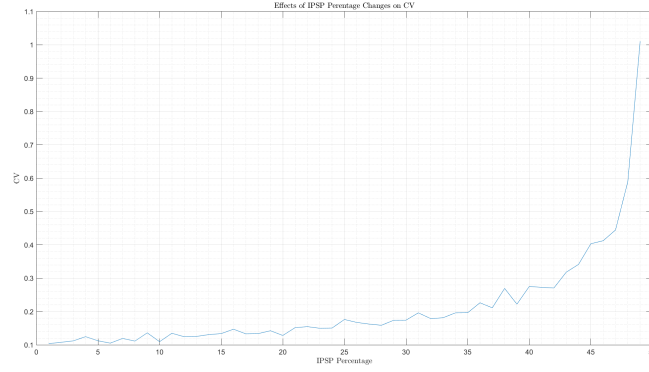


Figure 17: CV Changes Over Different Percentages Of IPSPs With Constant  $\tau_m$  and  $N_{th}$ .

5. To see the effect of the D ms window where a coincidence detector neuron needs to get N spikes out of M spikes, a simulation is done and can see the result in Figure 18. The bigger D, needs the bigger  $\frac{N}{M}$  to get fired. With bigger  $\frac{N}{M}$  in a specific D ms window, the CV is bigger than smaller  $\frac{N}{M}$ .

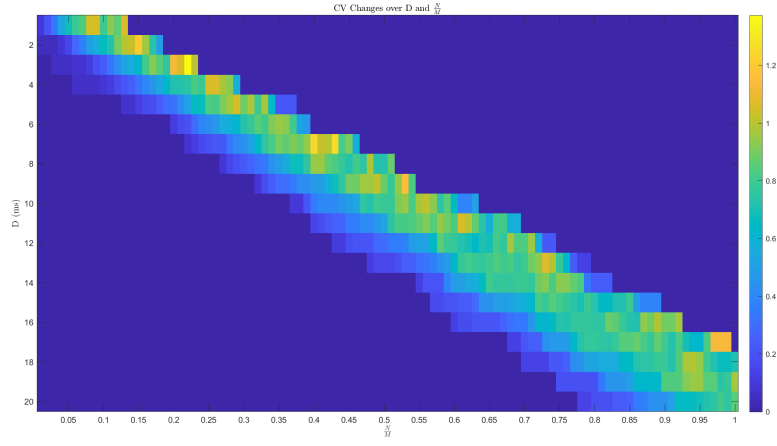


Figure 18: CV Changes Over Different Windows and  $\frac{N}{M}$ .

6. Here I try to add IPSP to see the effect of IPSP on CV in last section. As we can see in Figure 19, the same effect also can be seen here but there are two differences. One is for bigger range of D, we have a positive CV and in a constant D ms.

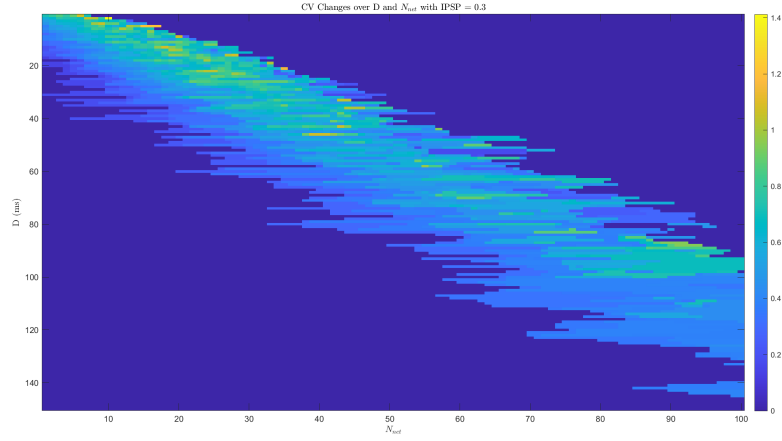


Figure 19: CV Changes Over Different Windows and  $\frac{N}{M}$  With IPSP.

## References

- [1] Softky WR, Koch C. The highly irregular firing of cortical cells is inconsistent with temporal integration of random EPSPs. J Neurosci. 1993 Jan;13(1):334-50. doi: 10.1523/JNEUROSCI.13-01-00334.1993. PMID: 8423479; PMCID: PMC6576320.
- [2] Michael N. Shadlen, William T. Newsome, Noise, neural codes and cortical organization, Current Opinion in Neurobiology, Volume 4, Issue 4, 1994, Pages 569-579, ISSN 0959-4388, [https://doi.org/10.1016/0959-4388\(94\)90059-0](https://doi.org/10.1016/0959-4388(94)90059-0).